From Research to Design in European Practice, Bratislava, Slovak Republic, on June 2 – 4, 2010

RAPID IMPACT COMPACTION FOR MIDDLE-DEEP IMPROVEMENT OF THE GROUND – NUMERICAL AND EXPERIMENTAL INVESTIGATIONS

Franz-Josef Falkner [1], Christoph Adam [2],
Ivan Paulmichl [3], Dietmar Adam [4], Johannes Fürpass [5]
[1, 2] University of Innsbruck, Technikerstr. 13/4, 6020 Innsbruck, Austria
[3, 4] GEOTECHNIK ADAM ZT GmbH, Wiener Str. 66-72/15/4, 2345 Brunn am Gebirge, Austria
[4] Vienna University of Technology, Karlsplatz 13, 1040 Vienna, Austria
[5] TERRA-MIX Bodenstabilisierungs GmbH, Schönaich 96, 8521 Wettmannstätten, Austria
[1] Dipl.-Ing., phone: +43 512 507-6731, e-mail: franz.falkner@uibk.ac.at
[2] Univ.Prof. Dr.techn., phone: +43 512 507-6585, e-mail: christoph.adam@uibk.ac.at
[3] Dipl.-Ing., phone +43 2236 312244-21, e-mail: paulmichl@geotechnik-adam.at
[4] Univ.Prof. Dr.techn., phone +43 2236 312244-11, e-mail: dietmar.adam@geotechnik-adam.at
[5] phone +43 3185 30722, e-mail: johannes.fuerpass@terra-mix.com

ABSTRACT: This paper presents results of numerical and experimental studies concerning the effect and efficiency of the Rapid Impact Compactor (RIC). The RIC is a dynamic compaction device for middle-deep ground improvement based on the piling hammer technology used to increase the bearing capacity of soils through controlled impacts. Theoretical investigations comprise numerical computer simulations of the impulse-type compaction effect, the energy transfer into the soil and the wave propagation. Experimental tests on different soil conditions provide the verification of theoretical analyses and the basis for the optimized and economic application of the compaction method in practice. Case studies of different construction projects demonstrate the successful application the RIC for middle-deep improvement and compaction of the ground.

1. Introduction

The Rapid Impact Compactor (RIC) is an innovative dynamic compaction device based on the piling hammer technology used to increase the bearing capacity of soils through controlled impacts. The general idea of this method is to drop a falling weight from a relatively low height onto a special foot assembly at a fast rate while the foot remains permanently in contact with the ground. At present in the Central European area there are some devices, which aim at closing the gap between the surface compaction methods (e.g. roller compaction) and the deep compaction methods (e.g. deep dynamic compaction/replacement) and permitting a middle-deep improvement of the ground.

The RIC consists mainly of three impact components: the impact foot, the driving cap, and the hammer with the falling weight. The impact foot made of steel has a diameter of 1.5 *m*. The driving cap connected to the foot allows articulation. Impact foot, driving cap, and falling weight are connected to the so-called hammer rig (see Fig. 1). Falling weights of mass 5000, 7000, 9000 or 12000 *kg* are dropped from a falling height up to 1.2 *m* at a rate 40 to 60 repetitions per minute [1].

The RIC provides middle-deep compaction up to a depth of 4 to 7 *m* in an efficient and economic way. The comparison to other dynamic compaction techniques with respect to the depth effect shows that the RIC is an ideal amendment between near-surface compaction

technologies (static and dynamic rollers) and deep compaction techniques (deep vibro compaction, vibroflotation and deep vibro-replacement, heavy tamping).

Gravels, sands, silts, industrial byproducts, tailings material, and landfills can be successfully compacted by the RIC, which can be used to increase the bearing capacity of foundations, to improve the ground bedding conditions for slabs, to reduce the liquefaction potential of soils, and to stabilize waste materials.

Data monitoring during the compaction process and the online display in the operator's cab enables compaction control, an economic application of the compaction tool, and a work integrated quality control. The total impact depth of the impact foot, the number of blows, and the final settlement of the impact foot after a blow define the stop code.

Fig. 1. Rapid Impact Compactor (left), impact foot with driving cap (center top), points of compaction (center bottom), and process of compaction (right).

2. Numerical Investigations

2.1 Mechanical Model

For the presented numerical investigations a simple mechanical model is utilized. The falling weight is modeled as lumped mass m_G. The velocity of the falling weight just before it strikes the impact follows the relation

$$v_G = \sqrt{2gh_0} \tag{1}$$

where h_0 is the falling height, and g represents the acceleration of gravity. The initial velocity v_F' of the impact foot is derived from v_G assuming an idealized elastic impact between falling mass m_G and impact foot of mass m_F according to [2]

$$v_F' = \frac{2m_G v_G}{m_G + m_F} \tag{2}$$

The soil medium is modeled as homogenous, isotropic, and elastoplastic halfspace. The axially symmetric impact foot made of steel rests on the surface of the halfspace. In the mechanical model a sliding interface between the foot and the soil is adopted, i.e. only normal stresses are transferred between the foot and the soil. The numerical model takes advantage of the rotational symmetry of this subsystem, which is divided into a near-field and a far-field. The near-field is discretized by means of Finite Elements. Infinite Elements model the far-field in order to avoid wave reflexions at the boundary between the near- and far-field, and to allow for energy propagation into the semi-infinite halfspace. Fig. 2 shows a sketch of the numerical model of the subsystem “impact foot – soil”.

Numerical simulations are conducted for a single impact and for a sequence of impacts. For the latter case a time lag of 1 *s* between the impacts is chosen.

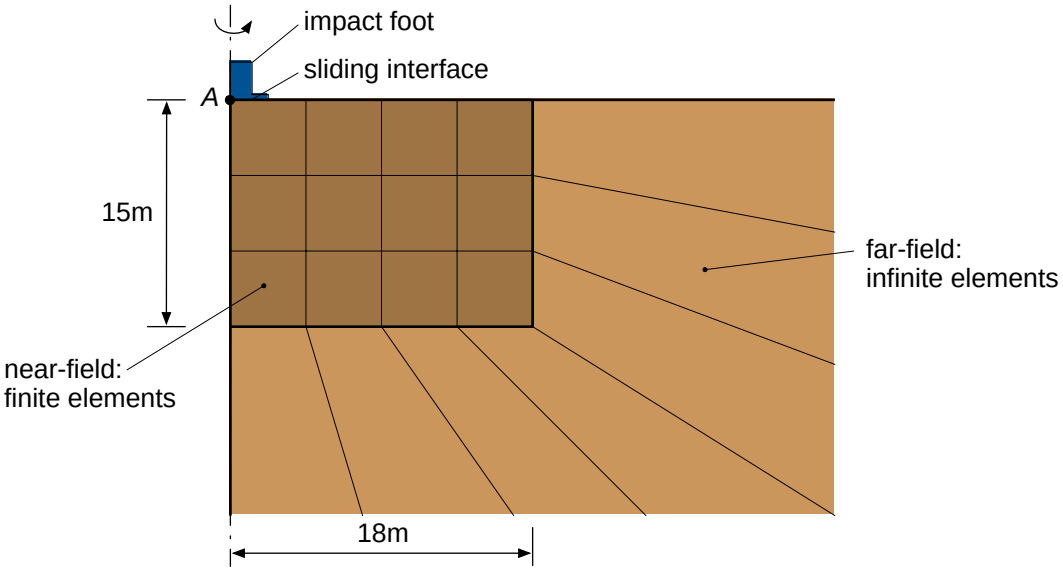

Fig. 2. Numerical model of the subsystem “impact foot - soil”.

All presented results are based on the following parameters: $h_0 = 1.2\,m$, $m_F = 4000\,kg$, $m_G = 9000\,kg$. For the subsoil the material properties of silty fine sand are employed assuming rate-independent plasticity without and with isotropic hardening [3]. These parameters are Young’s modulus $E = 10\,MN/m^2$, Poisson’s ratio $\nu = 0.3$, mass density $\rho = 2000\,kg/m^3$, cohesion $c = 5\,N/m^2$, friction angle $\phi = 26°$, and dilation angle $\psi = 8°$. 5% viscous damping of the underground at the fundamental frequency and at 70 *Hz* is considered according to Rayleigh [4].

2.2 Results

The global dynamic process in the subsoil can be evaluated considering the time history of the energy content in the subsystem “impact foot – soil”. Fig. 3(a) presents for the unlimited elastic soil the kinetic energy E_k, the energy radiation E_r at the boundary to the far-field, and the dissipated energy E_v by means of viscous damping. At $t = 0$ the kinetic energy E_{k0} of the impact foot is equal to the total energy of this subsystem. Viscous and geometric damping leads to a rapid decay of the kinetic energy. After 0.4 *s* the dissipated energy E_v remains almost constant. After 0.2 *s* primary waves approach the boundaries of the near-field. From this instant the infinite elements start to absorb energy, and E_r grows from zero. The more energy-rich shear and Rayleigh waves [5] meet the boundaries of the near-field at time $t = 0.4$ *s*, and the increase of E_r accelerates. At $t = 0.55$ *s* the system is at rest, $E_k = 0$, and E_v and E_r remain constant.

The kinetic energy E_k, and the energy dissipated by viscous damping and plastic deformation E_v and E_p respectively, of the elastoplastic soil are presented in Fig. 3(b). In contrast to E_k of the elastic soil here E_k drops continuously. Almost no energy is absorbed at the boundaries of the near-field because most of the energy is already dissipated in the near-field by plastic deformations and viscous damping. Energy E_p dissipated by plastic deformations is related to the compaction work. According to Fig. 3(b) less than half of the input energy is converted into compaction work. Viscous damping, which does not contribute to soil compaction, dissipates the remaining energy.

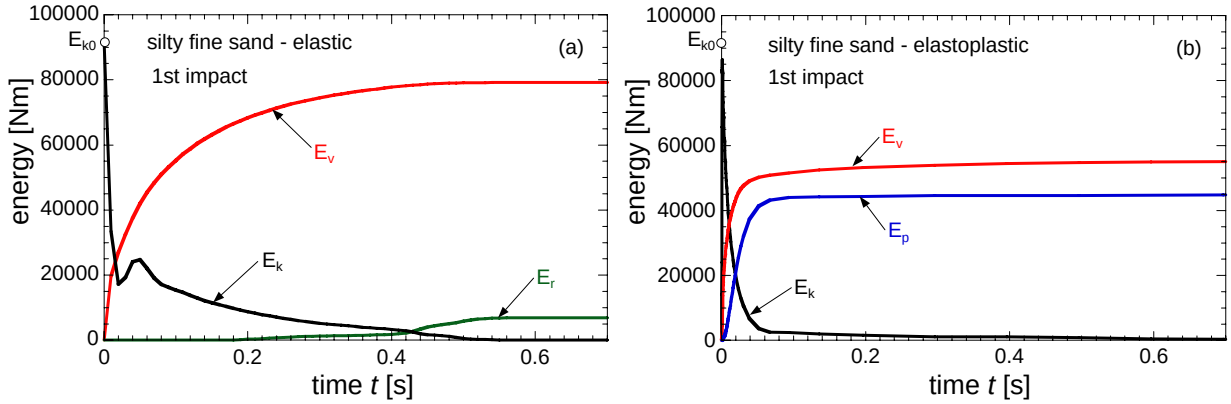

Fig. 3. Time history of the kinetic energy E_k, dissipated energy through viscous damping E_v, dissipated energy through plastic deformations E_p, and absorbed energy at the boundaries E_r. (a) Elastic response. (b) Elastoplastic response.

Fig. 4 shows the time history of the energy in the subsystem “impact foot – subsoil” during five consecutive impacts. In the corresponding numerical simulation isotropic hardening of the subsoil was assumed to hold true. This assumption allows the consideration of the increase of soil compaction after each impact. The spikes in the kinetic energy E_k correspond to the applied impacts. After each impact the rate of increase of energy dissipated by plastic deformations E_p drops because of isotropic hardening of the subsoil. Thus, viscous damping dissipates more and more of the input energy after each consecutive impact, and the RIC becomes less efficient.

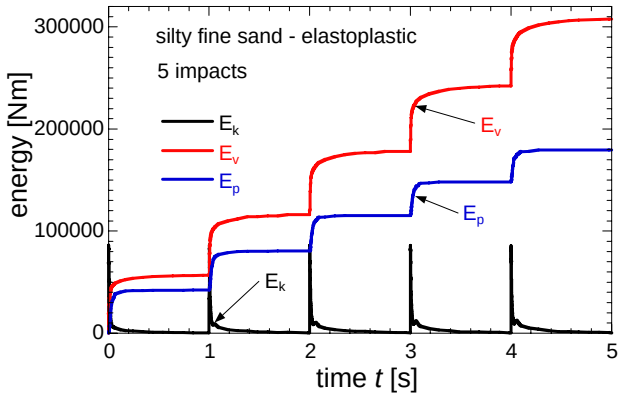

Fig. 4. Time history of the kinetic energy E_k, of the dissipated energy through viscous damping E_v, and of the dissipated energy through plastic deformations E_p after five consecutive impacts. Elastoplastic soil with isotropic hardening.

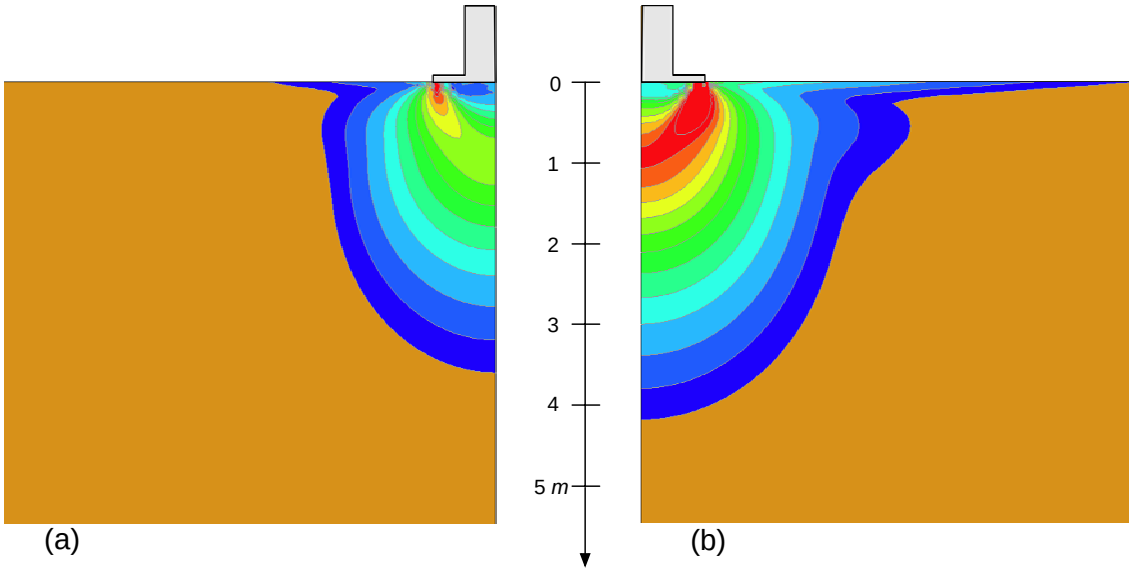

Fig. 5. Distribution of the equivalent plastic strain in the subsoil. (a) After the first impact. (b) After the fifth impact.

Furthermore, it is investigated up to which depth the RIC compacts the soil. Here, isotropic hardening of the subsoil models compaction of the soil. It is assumed that the equivalent plastic strain [6] is the characteristic parameter for evaluation of the compaction depth. A threshold of 0.02 separates the compacted space from the non-compacted subsoil. In Figs 5 colored areas correspond to equivalent plastic strains larger than the threshold mentioned above. Fig. 5(a) shows the compacted subsoil after the first impact, Fig. 5(b) after the fifth impact. These results verify for subsoils of silty fine sand a compaction depth of more than 4 *m*. The domains of equal plastic strains, i.e. the domains of equal degree of compaction, show the shape of an “onion”.

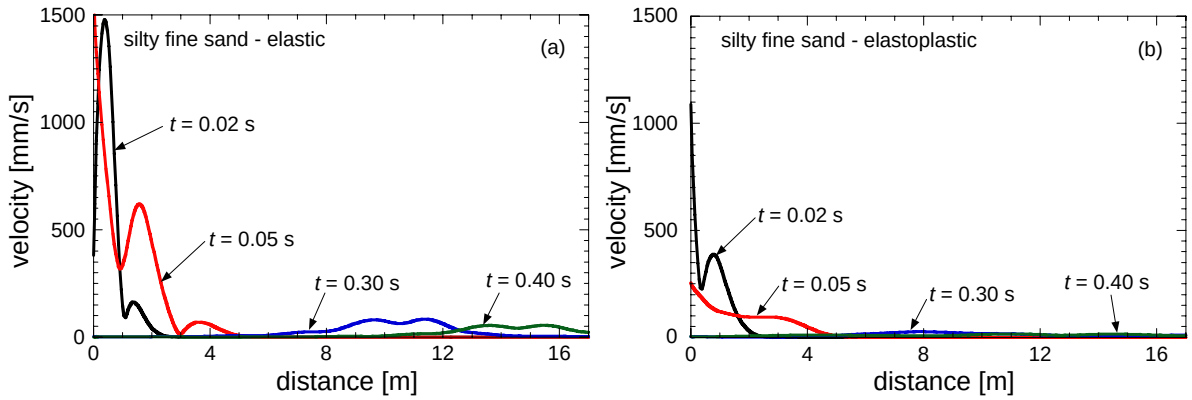

Fig. 6. Magnitude of resulting velocity for different instants as function of the distance from the impact foot. (a) Elastic response. (b) Elastoplastic response.

According to many provisions the magnitude of the resulting surface velocity is the characteristic response parameter for the assessment of the damage potential of ground motions on adjacent buildings and settlements. Thus, the application of the RIC in the vicinity of civil engineering structures requires a reliable estimation of this response quantity as a function of the distance from the compaction point. This quantity is evaluated from outcomes of the described numerical studies. At first, the dynamic response to a single impact on virgin soil is considered. Fig. 6(a) shows the magnitude of the resulting surface velocity at different discrete

time intervals after the impact. Shortly after the impact at $t = 0.02\ s$ the maximum magnitude of about 1.45 *m/s* emerges at a distance of 0.5 *m* from the edge of the impact foot. Another local maximum emerges at a distance of about 1.3 *m*. Geometric and viscous damping lead to a rapid decay of the velocity. E.g. at $t = 0.40\ s$ the maximum magnitude of the resulting velocity is just about 0.05 *m/s*. In Fig. 6(b) results from simulations taking into account soil compaction through inelastic deformations are depicted. Obviously, energy dissipation through plastic deformation reduces the magnitude of the resulting velocity at the soil surface considerably.

The decay of magnitude of the resulting velocity as function of the distance from the compaction point is shown in Fig. 7, where the maximum values at discrete surface points are plotted in logarithmic scale. In such a representation a linear regression line approximates the outcomes. In this figure the elastic response is set in contrast with the inelastic one. E.g. at a distance of 1 *m* of the edge of the compaction foot for the elastoplastic soil the maximum magnitude of the resulting velocity is 0.36 *m/s* compared to 1.79 *m/s* for the unlimited elastic underground. Additionally, this figure shows the maximum velocity after the 2nd and the 3rd impact applied to the elastoplastic soil. The difference to the response after the 1st is impact is insignificant. During the compaction procedure at a single point with 50 to 60 recurring impacts the maximum velocity will be increase slightly after each impact. Note that the regression line of elastic soil and the elastoplastic soil are almost in parallel.

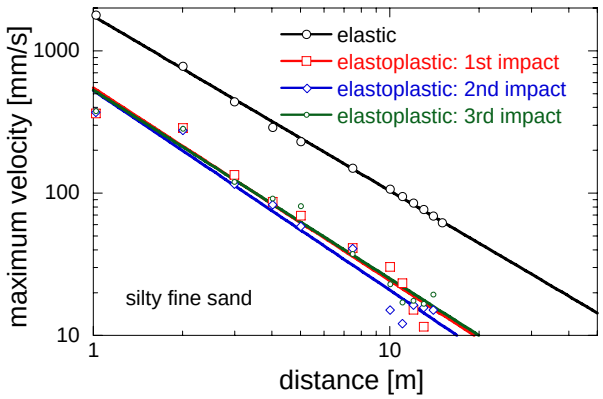

Fig. 7. Magnitude of maximum resulting velocity as function of the distance from the impact foot. Elastic and elastoplastic response after the first, second, and third impact.

Figs 8 show the spatial propagation of the resulting velocity at four instants after the first impact applied to the elastoplastic subsoil. The complete near-field, which is dicretized by means of Finite Elements, is depicted. The last figure verifies that the waves are not reflected at the boundaries to the far-field. Furthermore, it can be seen that the maximum velocities emerge on the soil surface. Thus, Rayleigh waves exhibit also in the elastoplastic soil the largest part of energy.

3. Experimental investigations

Large-scale tests on various test tracks and different ground conditions act as reference for verification of the numerical results. For these experimental investigations dynamic gauges are installed both in the ground and on the compaction tool in order to measure the vibration behavior of the total system and to compare the measured data with the results from numerical simulations. In addition, soil investigations are performed in-situ and in the laboratory. The analysis of the wave propagation is essential to evaluate the effect of dynamic compaction techniques on human beings and adjacent structures. Depending on soil type and set-up of device parameters the leading response quantity, which serves as basis for dimensioning the soil improvement works, need to be defined.

In the following section exemplary selected results of in-situ soil investigations are presented.

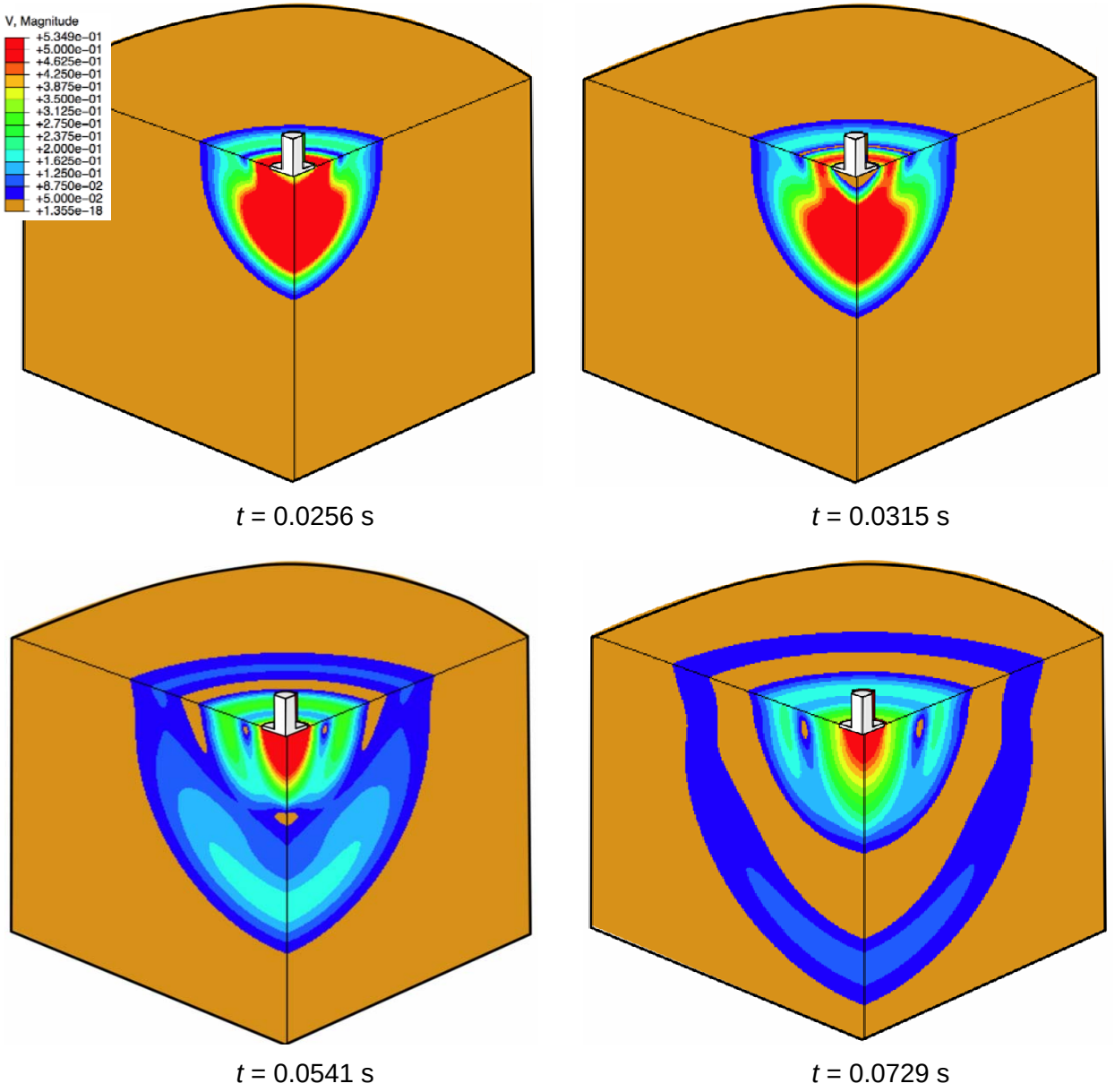

Fig. 8. Distribution of the magnitude of the resulting velocity (in m/s) at different instants. Elastoplastic soil.

3.1 Verification of compaction effect

Optimization and control of compaction with the RIC is assured by meeting the stop code criteria, GPS based compaction including work integrated documentation of the performance parameters for each compaction spot, and conduction of cone penetration tests and/or dynamic probing before and after compaction. During the compaction process the following stop codes are applied:

- Stop code 1: total settlement (depth of the compaction crater), e.g. > 0.8 *m*
- Stop code 2: number of blows per compaction point, e.g. > 50
- Stop code 3: final settlement of the last blow, e.g. < 10 *mm*

These stop codes are previously verified and optimized on a test site. The compaction parameters

- number of blows,
- final settlement at the last blow,
- total settlement (depth of the compaction crater),
- compaction energy, and
- average number of blows,

as well as coordinate of the compaction points, date, and time are monitored electronically for each compaction point during the compaction process and automatically documented via GPS controlled data acquisition.

Thus, local heterogeneities can be clearly identified and the compaction with the RIC can be adjusted systematically. If necessary, additional compaction passes are conducted.

For determination of the compaction depth cone penetration tests (CPT) and/or dynamic probing light, medium, or heavy (DPL, DPM, or DPH) are carried out.

In Figs 9 number of blows N_{10} determined by dynamic probing heavy (Fig. 5(a)) and light (Fig. 5(b)) before and after compaction is plotted against the depth. The dynamic probing heavy was performed in non-cohesive primarily sandy gravelly soil, the dynamic probing light was carried out in cohesive soil consisting of silts and sands. It can be seen that the depth effect of the RIC depends on the soil condition, and it varies from about 4 *m* (silts and sands) to 7 (8) *m* (sandy gravelly soils).

In cohesive soils of soft to stiff consistency dynamic probing heavy allows only a low number of blows independent of the degree of compaction. Consequently, for checking the compaction effect it is recommended to use dynamic probing light (DPL) or cone penetration tests (CPT) [7].

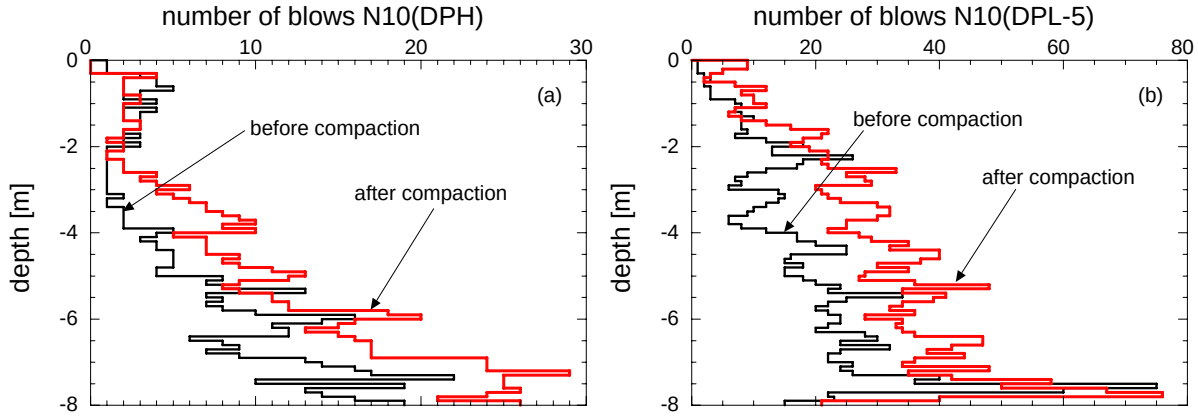

Fig. 9. (a) Number of blows N10 before (black) and after compaction with the RIC (red). Dynamic probing heavy (DPH) in non-cohesive soil. (b) Dynamic probing light (DPL-5) in cohesive soil (right).

In Figs 10 the results of CPT before and after soil compaction with the RIC are shown. The considered subsoil consists of silty layer of about 4 *m* thickness, which rests on alluvial gravel deposits from the river Danube. From the distribution of the base resistance (Fig. 10(a)) a compaction effect of about 4.5 to 5 *m* depth can be identified. According to experience sandy soils allow deeper compaction than silty soils. Figs 10 reveal that the upper alluvial gravelly deposits below the silty layer were compacted as well.

The low degree of compaction in the top domain of 1 to 1.5 *m* depth can attributed to the fact that the compaction crater of the RIC was filled with non-compacted extraneous material. Usually, after filling the compaction crater this material is compacted by a heavy dynamic roller.

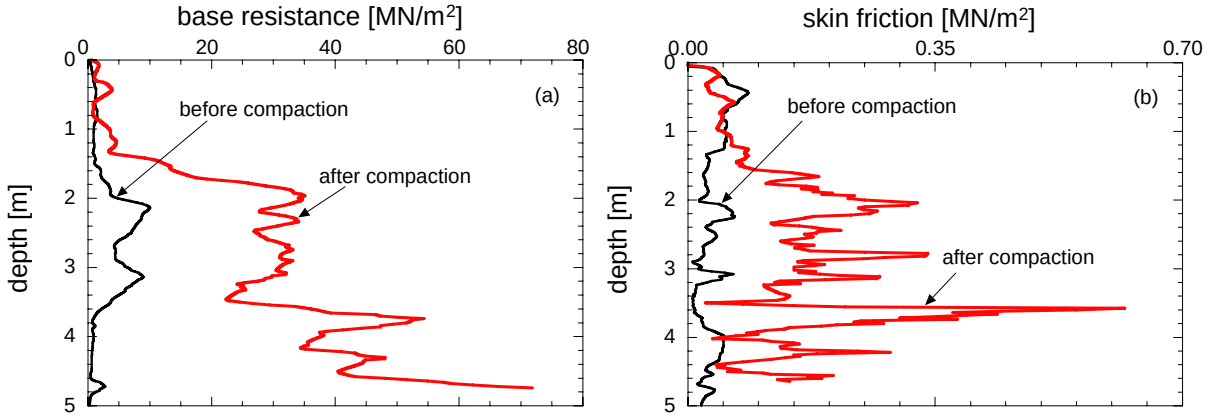

Fig. 10. Cone penetration tests (CPT) in cohesive soil before (black) and after compaction with the RIC (red). (a) Base resistance. (b) Skin friction.

3.2 Vibration measurements

On numerous test sites maximum surface velocity induced by the RIC as function of the distance were determined. The data acquisition tool MR2002DIN-CE (RED BOX) of company SYSCOM was applied to monitor and record these vibrations. The velocities were measured in situ with tri-axial velocity transducers according to the German Standard DIN 45669 (SYSCOM, type MS2003 A3HV 315/1) and a data recorder (SYSCOM, type MR2002 DIN-CE). The velocity was measured in three orthogonal directions in the frequency domain of 1 to 315 Hz. The subsequent data processing was done with the software package VIEW 2002 (Ziegler Consultants). Subsequently, regression analyses were performed to obtain the magnitude of the maximum resulting velocity $v_{R,max}$ as function of the distance from the impact foot.

Fig. 11 shows selected regression lines for different ground conditions. Lowest values of velocity develop during compaction of loose sandy gravels. For this subsoil condition a coefficient of decay of about 1.8 was determined. It is noted that only one compaction pass was performed and the intensity of vibration increases with increasing passes [7]. Largest values of velocity were measured during compaction of dense gravels. Compaction of sandy silts and gravelly silty sands led to velocities in-between. The coefficient of decay of about 1.3 is practically identical for dense gravels, sandy silts, and gravelly silty sands.

The maximum limit value of zul $v_{R,max}$ = 10 *mm/s* for building classification No III according to the Austrian Standard ÖN S 9020 is under-run at a distance of 11 to 34 *m* from the impact foot depending on the ground condition and soil type. Based of hitherto experience the required minimum distance to buildings of classification No III is about 20 *m*. In comparison compaction of heavy tamping techniques induces resulting velocities of more than 10 *mm/s* at a distance of 30 *m*.

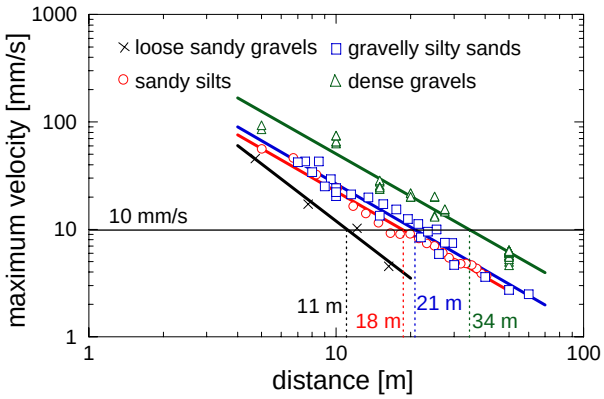

Fig. 11. Magnitude of maximum resulting velocity as function of the distance from the impact foot. Measured values for different soil types.

3. Conclusions

Results from numerical and experimental investigations performed with the Rapid Impact Compactor (RIC) are compared and discussed. The compaction depth effect of more than 4 *m* for silty fine sand derived from numerical simulations confirms the depth effect of at least 4.5 to 5 *m* measured in field tests, which can be up to 7 (8) *m* depending on ground condition and soil type. The maximum resulting surface velocity as function of the distance from the impact foot determined numerically and in-situ are in the same order of magnitude. Thus, the precision of mechanical modelling for the numerical studies could be verified for the parameter range considered in the scope of the performed investigations.

Acknowledgement

The Austrian Research Promotion Agency (FFG) has funded this research project. This support is gratefully acknowledged.

Literature

[1] Adam, D.; Paulmichl, I.: Impact compactor – an innovative dynamic compaction device for soil improvement. Proc. 8th International Geotechnical Conference (June 4-5, 2007, Slovak University of Technology, Bratislava, Slovakia), pp. 183-192, 2007.

[2] Ziegler, F.: Mechanics of Solids and Fluids. 2nd edition, corr. 2nd printing. Springer Vienna New York, 1995.

[3] Muir Wood, D.: Soil Mechanics and Critical State Soil Behaviour. Cambridge University Press, 1991.

[4] Chopra, A.K. (2006) Dynamics of Structures. 3rd ed. Prentice Hall, New Jersey.

[5] Verruijt, A.: An Introduction to Soil Dynamics. Springer Dordrecht, 2010.

[6] ABAQUS Theory Manual, Version 6.5-1, 2004.

[7] Paulmichl, I.; Fürpass, J.: Mitteltiefe Bodenverbesserung mit dem Impulsverdichter – Fallbeispiele aus der Praxis. Proc. 7th Österreichischen Geotechniktagung (January 21-22, 2009, Vienna), in German, pp. 341-352, 2009.